

Fractures and rock properties estimated by 3D directional borehole radar

K. Wada¹, S. Karasawa², K. Kawata³ and S. Ebihara⁴

^{1,2,3}Matsunaga Geo-Survey Co., Ltd., Tokyo, JAPAN

kazuwada@m-gs.co.jp

⁴Osaka Electro-Communication University, Neyagawa, JAPAN

s-ebihara@m.ieice.org

Abstract— Borehole radar is widely used in civil engineering work such as fault and fracture exploration, salt dome investigation, tunnel detection, UXO detection, exploring locations of foundation piles and sheet metal piling walls, and so on. Borehole radar surveys in resistive rock field have been applied successfully due to the lower attenuation of the rock media. Through those studies, many researchers have become interested in the detectability of thin open fractures and their locations. Though there are some numerical computing studies [1] on its detectability related to the open widths of fractures, there are very few experimental field studies. Thus studies using directional borehole radar system are essentially required at borehole sites where geometrical features and open widths of the fractures are well investigated.

We are conducting experimental evaluation surveys for our 3D directional borehole radar system, “ReflexTracker[®]”. In soft ground in an alluvial plain, a single-hole measurement was carried out to evaluate the detection ability of a conductive cylinder buried 2m from the survey hole and found that the system could detect 3D reflectors representing the target and provided information on the direction of arrival wave and distance to the target [2].

We conducted another experimental measurement to evaluate fracture detectability of the system in rock field. The experimental borehole (BOA-200), a vertical borehole with diameter of 86-115 mm reaching 200 m depth in andesite rock, is located in a rock quarry in Ishikoshi Town, Miyagi Prefecture, Japan. Fractures in the borehole and their geometrical features such as strikes, dips and open widths were investigated in detail by borehole scanner [3], and the electrical characteristics were also obtained by a logging survey for all depths.

The radargrams obtained by the non-directional antenna indicate that the arrival times and amplitudes were clearly related to rock mass classification and fracture densities, i.e., the higher the density, the larger the amplitude and the earlier the arrival time. Moreover, interpreted relative permittivities were negatively correlated with resistivities. On the other hand, the interpreted 3D reflectors derived from the directional antenna resulted in significantly good fitting with some of the known fractures’ extended planes. Through the experimental study in the rock field, the ReflexTracker shows high potential for applications in fracture extractions and rock property investigations.

Keywords—*Directional Borehole Radar; ReflexTracker; dipole antenna; 3D; fracture; rock property; reflected wave*

I. INTRODUCTION

When constructing a large-scale underground facility in rock, exploration of faults and fractures is important for evaluating water paths and rock stability. For example, since faults and fractures may be water paths causing leakage of radioactivity in a radioactive waste site, they should be located and imaged. For this purpose, a tomographic image of the faults and fractures can be obtained with cross-hole borehole radar data. Since water-permeable faults and fractures reflect electromagnetic waves, they can be measured by single-hole borehole radar. Most conventional borehole radar systems for single-hole application use two vertical dipole antennas, which are omnidirectional. However, to estimate objects such as fractures and faults in 3D space with a single borehole, a directional borehole radar system is needed.

II. DIRECTIONAL BOREHOLE RADAR SYSTEM

We utilized “ReflexTracker”, a small-diameter 3D directional borehole radar system, in this experimental survey. This is a step frequency radar system with a wide frequency band between 5 kHz and 600 MHz, controlled by a vector network analyzer (VNA) which enabled us to calibrate all the cables’ delay and attenuation in the radar system. The directional-antenna probe was equipped with “Micro Electro Mechanical Systems” (MEMS) sensors to monitor rotation and tilt angles of the probe. This leads to precise estimation of the azimuth direction of the arriving wave, based on the arrival time difference in the time domain by the six dipole array antennas. All the data acquired by the radar probe with a diameter of 57 mm were transmitted to the surface equipment immediately via optical cable links. The surface equipment consisted of a surface control device, a personal computer and a portable VNA [2]. Moreover, we used a non-directional antenna probe in this system to observe relative permittivity.

III. EXPERIMENTAL STUDY

A. Site explanation

We took experimental measurements to evaluate the fracture detectability of the system in a rock field. The experimental borehole, BOA-200, a vertical borehole with diameters of 150 mm to 50 m depth and 86 mm down to 200 m in andesite rock, is located in a rock quarry in a hilly area at 42 m a.s.l. in Ishikoshi Town, Miyagi Prefecture, Japan (Fig.

1). This area is underlain by Ishikoshi andesite rocks of the Miocene. The andesite rock consists of dacite, andesitic lavas and volcanic breccia. The borehole penetrated homogeneous andesite rocks.

Fractures in the borehole and their geometrical features such as strikes, dips and open widths were investigated in detail by a borehole scanner [3], and the electrical characteristics of the rock were also obtained by a logging survey for all depths.



Fig. 1. Study site in the rock quarry.

B. Measurement of non-directional borehole antenna

Measurement by non-directional borehole antenna was conducted at 10 cm intervals in two depth ranges of 5 to 15 m and 53 to 57 m. We estimated electromagnetic wave velocities using observed travel times of the direct waves from a transmitter antenna (Tx) to a receiver antenna (Rx) and converted them to relative permittivities. Obtained relative permittivities were used to observe in detail near and above the underground water level and to compare with fracture densities.

Depth range of 5 to 15 m

Since a water level located at a depth of 14.7 m, the feeding points of the Rx and Tx antennas of the ReflexTracker would be located near the underground water level in the measurement of this depth range. The depth of the water level did not change during the measurements. We tried to estimate relative permittivities at probe depths in this transition area, separating it into the four zones shown in Table I, by considering the antennas' depths and the water level. In order to calculate the correct relative permittivities, we first estimated the preliminary relative permittivities from the direct wave's propagation velocities and constructed simulation models assuming the relative positions of Tx and Rx antennas and the water level and diameters of the probe, and conducted numerical simulation using the MoM (Method of Moments) [5] varying the relative permittivities at the measured depths to fit calculated travel times to the measured travel times of the direct waves from Tx to Rx antennas.

In zones 1 and 4, we estimated relative permittivities in the models assuming Tx and Rx antennas in the air and water,

respectively. In zones 2 and 3, because the relative positions of antennas and water level varied at the measurement depths, we utilized models assuming that the Tx and Rx antennas were located in the air and water, respectively (Fig. 2). Estimated average relative permittivities in host rock were 7.4 above the water level, and increased by 30 % to 9.8 under the water level. The sharp rise of the relative permittivities in the uppermost part of zone 2 might have been caused by the differences between the models and field measurement conditions. Whereas the average relative permittivity was around 7.3 at depths of less than 10.5 m in zone 1, the average one was 7.8 at the deeper depth. The reason for this may have been that the fracture density in the upper part of zone 1 was lower than that of lower part.

TABLE I. MEASUREMENT SITUATION FOR FEEDING POINTS OF TX AND RX ANTENNAS AROUND THE DEPTHS OF THE GROUNDWATER LEVEL.

Zone	Bottom depth (m)	Measurement		Simulation		Relative permittivity
		Tx	Rx	Tx	Rx	
1	12.9	air	air	air	air	7.4
2	13.9	water	air	water	water	10.1
3	14.7	center in water		water	water	10.0
4	-	water	water	water	water	9.8

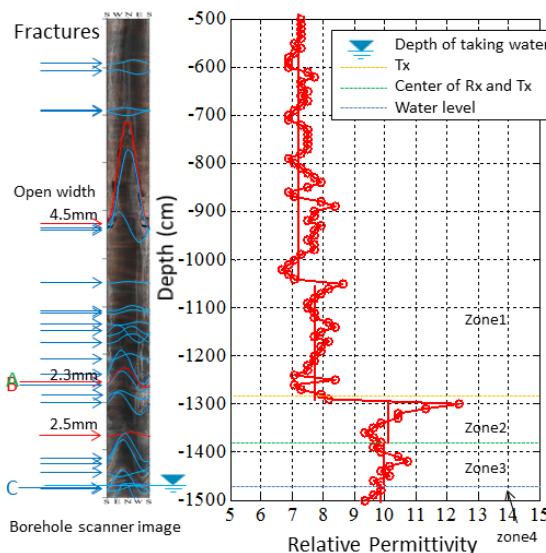


Fig. 2. Relative permittivity around water level.

Depth range of 53 to 57 m

At this depth range, rock mass properties vary from class-CH (relatively hard rock quality) in the upper layer of the 53.1m depth, with high fracture densities to Class B (hard rock quality) in the lower layer with sparsely distributed fractures (Fig. 3). Our measurements were targeting mainly host rock with the rock mass classification of B. The upper part of the survey range was affected by a layer with high fracture density.

The radargrams obtained by the non-directional antenna indicate that the arrival times and amplitudes are clearly related to rock mass classification and fracture densities, i.e., the higher the density, the larger the amplitude and the earlier the arrival time.

On the other hand, general features of resistivities obtained by electrical logging measurement indicate that it ranged from around 50 Ω m to more than 100 Ω m with depth, with a dramatic increase at the depth of 55 m. The interpreted relative permittivities are negatively correlated with resistivities.

Phases and amplitude features of the radargrams as described above clearly indicate electric characteristics of the host rock which is difficult to interpret only by observation of rock samples and fracture distributions, and is a simple and appropriate approach that is suitable for the estimation of rock properties.

C. Measurement of directional borehole antenna

To estimate the 3D geometrical distribution of fractures, we observed radar signals using the directional borehole probe with 6-element array antennas. Fig. 4 shows the radargram obtained at the depth range of 5.50 to 14.5 m. Many characteristic phases can be seen with earlier arrival times with the depths and might be reflected waves from fractures.

We choose three representative phase groups, named phase 1 (Ph1), phase 2 (Ph2) and phase 3 (Ph3), as phase candidates for 3D reflected point estimations. To detect 3D features of fractures, we utilized Ebihara's algorithm [4]. The interpreted 3D reflectors derived from the directional antenna resulted in significantly good fitting with some of the known fractures' extended planes based on the borehole scanner observation (Fig. 4).

The estimated 3D features of the reflected points are shown in Fig. 5 with the three interpreted fracture planes obtained by the borehole scanner observation. The green, red and blue circles represent the points reflected by the phases Ph1, Ph2 and Ph3, respectively. The corresponding fracture's characteristics interpreted from the borehole scanner imagery are also shown in the bottom of Fig. 5. As shown in Fig. 4, many fractures were obtained by the borehole scanner with geometrical features such as strikes and tilts of fractures and width of open cracks.

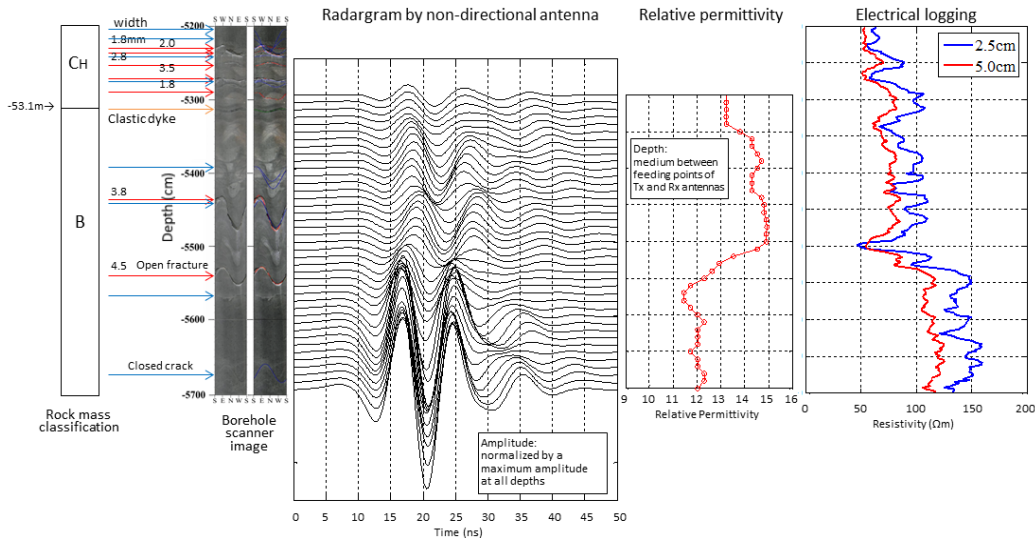


Fig. 3. Radargram with fracture distribution, estimated relative permittivity and electrical logging data.

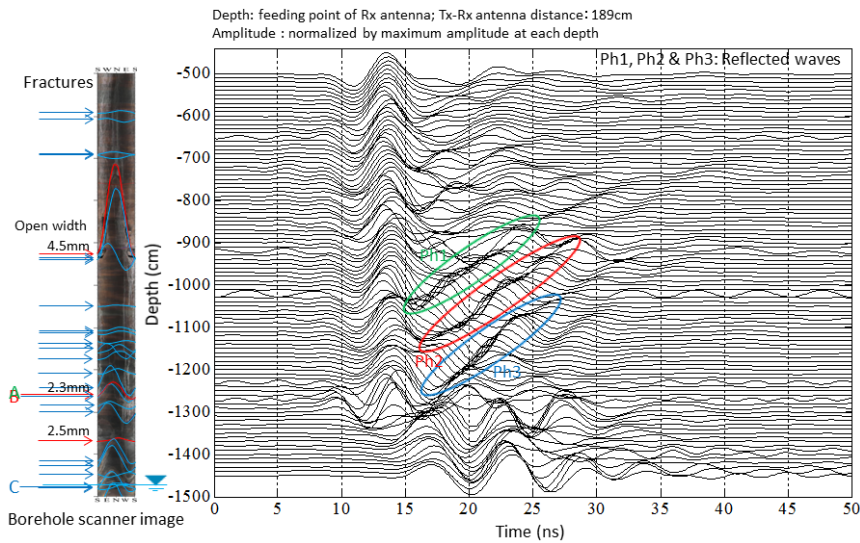


Fig. 4. Radargram obtained near the water level of borehole.

The three estimated reflected point groups with the corresponding fracture planes from the borehole scanner are shown in 3D space and on the fracture planes (Fig. 6 and Table II). The estimated reflected points are determined on the planes of the observed fractures, i.e., fractures A, B and C shown in Fig. 5. Our non-directional and directional borehole radar measurements revealed the rock properties of the host rock and 3D fracture distributions from a single-hole measurement configuration.

Through the experimental study in the rock field, the ReflexTracker shows high potential for application in fracture extractions and rock property investigations.

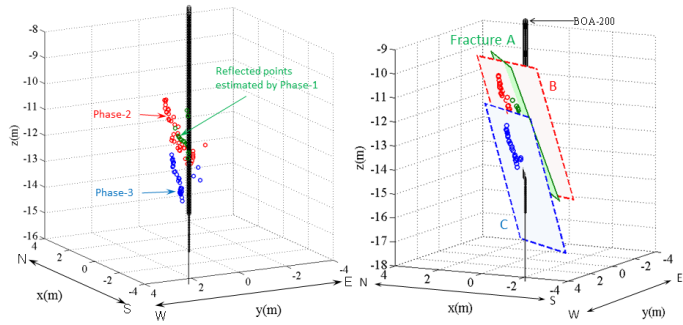


Fig. 5. Estimated 3D reflectors and their corresponding fractures

TABLE II. PHASES FOR 3D REFLECTED POINT ESTIMATION AND THE CORRESPONDING CRACKS FROM BOREHOLE SCANNER OBSERVATIONS

Fracture name	Used phase	Upper and lower depth (cm)	Strike and dip angles	Width of crack (mm)
A	Phase 1	1228 - 1267	N51E70S	2.3
B	Phase 2	1233 - 1274	N25E71E	0.0
C	Phase 3	1440 - 1488	N35E74E	0.0

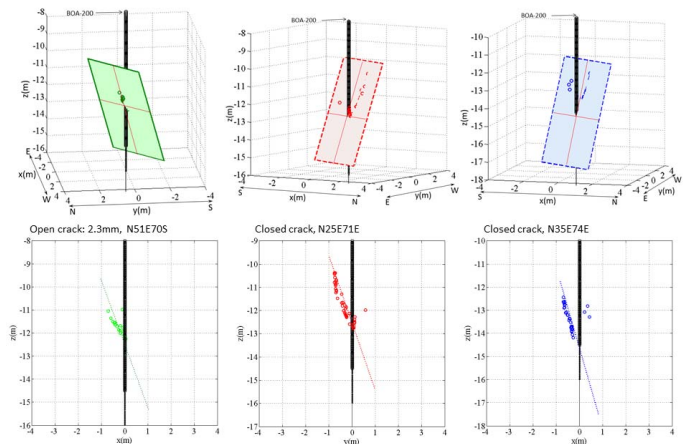


Fig. 6. Comparison between estimated 3D reflected points and fracture geometries

IV. CONCLUSIONS

1) Observing the arrival times of direct wave using a non-directional antenna probe and performing the MoM's

modeling calculation, we estimated detailed relative permittivity changes above and near water levels in the borehole at 10 cm intervals ranging from 5 to 15 m in depth. It revealed that though the relative permittivity changes depending on the fracture densities above the water level, they generally increase with depth and sharply rise at around 1.8 m above the water level. Moreover, the estimated relative permittivities ranging from 53 to 57 m in depth, which were below the water level, were inversely correlated with the resistivities, and rocks identified in the same rock mass classification showed a significant change in the depth range. These findings indicate that relative permittivity is a useful means for evaluating rock properties.

2) At a depth range from 5 to 15 m, we obtained three-dimensional locations of the reflectors using three remarkable reflected wave phases observed by the directional dipole array antennas. The reflectors' distribution indicates very good fitting with the extended portions of some existing fractures observed by a borehole scanner, but they are not necessarily open cracks in the borehole face.

3) Finally, we could confirm the applicability of our 3D directional borehole radar system, ReflexTracker for detecting fractures and revealing rock properties in homogeneous andesite rock field through the single-hole measurement configuration.

Acknowledgments

This work was supported by "3D-Directional Borehole Radar System", financed by "ASTEP: Adaptive and Seamless Technology Transfer Program Through Target-driven R&D" of the Japan Science and Technology Agency. We would like to thank Mr. Takayuki Sasaki of Boa Corporation for providing his borehole test site, BOA-200, for this survey. We would also like to acknowledge our colleagues Mr. Takashi Ueki for conducting electric well logging measurement, and Mr. Kyohei Yamada for supporting field operation of the ReflexTracker.

References

- [1] S. Liu, X. Chang, and L. Ran, "Analysis of fractures detectability by borehole radar," Proceedings of the 15th International Conference on Ground Penetrating Radar GPR2014, pp. 962-965, Brussels, 2014.
- [2] K. Wada, S. Karasawa, K. Kawata and S. Ebihara, "Small-diameter directional borehole radar system with 3D sensing capability", Proceedings of the 15th International Conference on Ground Penetrating Radar GPR2014, pp. 852-856, Brussels, 2014.
- [3] Tohoku Bureau of Ministry of Economy, Trade and Industry, "FY2011: Framework for supporting of strategic upgrading base technology on development of practical usage for low-cost borehole scanner system embedded depth recorder using image-sensor, Report on Drilling Borehole for Observation Circumstance Implementation", in Japanese, 2012.
- [4] S. Ebihara, H. Kawai and K. Wada, "Estimating 3-D position and inclination of a planar interface with directional borehole radar," Near Surface Geophysics, vol. 11, pp. 185-195, 2013.
- [5] S. Ebihara, A. Sasakura and T. Takemoto, "HE₁₁ mode effect on direct wave in singlehole borehole radar," IEEE Transaction on Geoscience and Remote Sensing, vol. 49, no. 2, pp. 854-867, Feb. 2011.